Heliyon 9 (2023) e13500

Contents lists available at ScienceDirect

Heliyon

journal homepage: www.cell.com/heliyon

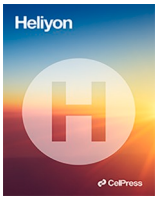

Research article

Transforming micropores to mesopores by heat cycling KOH activated petcoke for improved kinetics of adsorption of naphthenic acids

Oliver K.L. Strong [a], Elmira Nazari [a], Tyler Roy [a], Kevin Scotland [a], Paul R. Pede [b], Andrew J. Vreugdenhil [a,*]

[a] Material Science, Department of Chemistry, Trent University, 1600 West Bank, Peterborough, Ontario K9L 0G2, Canada
[b] Carbonix, 690 Mountain Rd, Suite 200, Fort William First Nation, Ontario P7J 1G8 Canada

ARTICLE INFO

Keywords:
Activated carbon
Petroleum coke
KOH
Mesoporosity
Naphthenic acid

ABSTRACT

Formation of activated carbon from petroleum coke by KOH, results in high specific surface area materials that are predominantly microporous. This initial microporosity means that the adsorption kinetics of target species are not as rapid as they could be, thus limiting environmental remediation applications for the material. To address this problem a series of additional heat cycles with no additional chemical inputs were applied after activation but prior to the removal of activating agents. This process resulted in the oxidation of residual potassium metal from the initial activation which allows it to function again as an activating agent for the subsequent cycles. The heat cycling resulted in an increase in mesoporosity by 10–25% with each successive cycle independent of the KOH to feedstock ratio. This was shown to be demonstrably different than equivalently extended heating times, thus identifying the importance of thermal cycling. Adsorption kinetics of three model naphthenic acids showed faster kinetics for the pore widened activated carbon. The $t_{1/2}$ times dropped from 20 to 6.6 min for diphenyl acetic acid, 34.3 to 4.5 min for cyclohexane acetic acid, and 51.4 to 12.0 min for heptanoic acid.

1. Introduction

Activated Carbon (AC) is a porous carbonaceous material used for a variety of applications, from adsorption substrates for environmental remediation to electrodes and supercapacitors [1]. Common feed sources for AC include bituminous coal [2], and biomass wastes, such as coconut shells [3] and fruit pits [4]. The type of feedstock, along with the activating method and conditions, influences the pore size distribution, total specific surface area, pH, and surface functionality [5]. For biomass wastes, variations in cellulose, lignin and hemicellulose content are important in the formation of pores and surface functionality of produced AC. For coals and cokes, the carbon, oxygen and heteroatom content influences these textural and chemical properties.

In our research group, we investigate the potential utilization of petroleum coke (petcoke) for generating adsorbent carbon materials with particular application in environmental remediation. As petcoke is a substantial byproduct of the surface mining Alberta oil sands production, the generation of an effective and commercially viable environmental remediation material from this byproduct with potential direct application to water quality challenges related to oil sands production is clearly a potentially interesting area of

* Corresponding author.
E-mail address: avreugdenhil@trentu.ca (A.J. Vreugdenhil).

https://doi.org/10.1016/j.heliyon.2023.e13500
Received 19 January 2023; Received in revised form 26 January 2023; Accepted 1 February 2023
Available online 8 February 2023

investigation. Petcoke is typically over 85% carbon with 5–7% sulphur content which impedes more traditional uses in steel production [6]. As of 2011, over 72 million tonnes of petroleum coke had been stockpiled with inventories expected to go up year over year [5]. The high carbon content and abundance makes it a natural target for activation. Importantly, petcoke feedstocks activated by KOH have substantially higher yields than KOH activated lignocellulosic materials which makes the multiple cycle KOH activation described here ideal for petcoke but impractical for lignocellulosic feedstocks.

The key textural parameters for the behaviour of activated carbons are the specific surface area typically measured by nitrogen adsorption using BET models in m^2/g and the pore size distribution usually determined by DFT modelling of the adsorption and desorption isotherms of gaseous nitrogen or argon on the material surface. The significance of specific surface area is obvious for activated carbons, however the pore size distribution is often underreported and yet is a major factor in determining the kinetics of adsorption. Specifically for petroleum coke feedstocks, the majority of the specific surface area is derived from microporosity (<2.0 nm) with an inadequate distribution of mesoporosity (2.0–50 nm). In this work, we will describe a convenient and cost-effective method for controlling pore size distribution and demonstrate its utility for adsorption of naphthenic acids from oil sands process affected water (OSPW).

Chemical activation of petroleum coke with KOH has resulted in highly microporous activated carbons. This can create a bottle neck for the adsorption of analytes onto the activated carbon surface. As such, there is a body of work that has focused on widening the pores produced from the activation of petcoke; methods such as steam, hard templating [7], CO_2 activation, during or after KOH heat treatments, and the use of NaOH and K_2CO_3 [8] have all been applied to introduce additional mesoporosity [9,10]. These have mostly resulted in lower total surface areas with much lower yields. Hill et al. [11] saw large increases in mesoporosity of their 3:1 KOH: petcoke activated carbons when steam was introduced during activation, however the yields dropped from 80% to less than 10% [11]. Kugatov et al. [12] mixed carbon black with petroleum pitch and roasted it at high temperatures before activation with steam resulting in an activated carbon where the increasing mesoporosity had a linear relationship to declining yields. The improved mesoporosity they achieved had a reduced specific surface area of 300 m^2/g with a 70% mass loss. Jingfeng Wu et al. [13] had much more success with coactivation of petroleum coke with steam and KOH. Here yields were above 40% and total pore volume increased as pores widened to up to 4 nm after steam exposure. Min Yan et al. [14] improved the mesoporosity and hydrophobicity of activated carbon fibers by an additional 2:1 KOH activation with a nickel catalyst. Other works have focussed on mitigating the corrosive effects on machinery by limiting the amount of activating reagent through the addition of KCl which promotes the solubilisation of secondary products increasing the efficiency of the reaction and resulting in increased total pore volumes if not specifically mesoporosity [15]. Clearly these are promising results, but for scale up additional reagent could be prohibitive and the combination of steam, potassium hydroxide and high temperatures results in degradation of equipment and therefore higher costs. The aim of this research was to increase the mesopore volume of the largely microporous KOH activated petroleum coke and subsequently the kinetics of naphthenic acid adsorption, without increasing chemical inputs in the activation process. To increase mesoporosity in our petroleum coke activated carbon, we put the unwashed product through a heat cycling process. This cycling allows the potassium metal that forms under the reductive conditions of activation to oxidize and react within any pores that have formed in subsequent cycles. Initial work with cycling of a 1:1 mass ratio showed large increases in mesoporosity with small drops in yields and little change to specific surface areas. To explore the pore widening phenomenon further, an increased range of temperatures and impregnation ratios were explored.

The kinetics of adsorption of three model naphthenic acids (NA) was used to test the efficacy of the increased mesoporosity of pore widened activated carbon (PWAC). The term ‘‘naphthenic acid’’ is used to describe a broad distribution of polar organic carboxylic acids that occur naturally in petroleum [2,16] (insert Treatment of naphthenic acids in oil sands process affected water). NAs are known as the main organic environmental toxins in oil sands process affected waters (OSPW) which can cause serious problems to a wide range of organisms, the refining process, and underground and surface water resources [17]. They contain a complex mixture of alkyl-substituted acyclic and cycloaliphatic carboxylic acids, with the general chemical formula $C_nH_{2n+z}O_2$ where n indicates the carbon number and Z specifies the hydrogen deficiency resulting from forming ring structures [18]. The absolute value of Z divided by 2, gives the number of rings in the compounds. NAs can react with the salts present in OSPW and produce complexes which can result in corrosion in boilers and refining infrastructure [19,20]. As NAs are the major source of toxicity of OSPW with its associated risk of contamination of underground and surface water resources; these species serve as good candidates for testing the process water remediation efficacy of PWAC [21,22].

2. Methods

2.1. Materials

Petroleum coke from oil sands as provided by Suncor Energy Inc. Calgary Alberta, Canada was used as the feedstock for KOH activation. KOH and the naphthenic acids: diphenyl acetic acid (DPA), cyclohexane acetic acid (CHA), and heptanoic acid (HA) were purchased and used as received (Sigma Aldrich, Milwaukee, WI, USA).

2.2. Activation of petroleum coke with KOH and subsequent cycling experiments

Petroleum coke (PC) was ground to particle sizes less than 0.308 mm and pretreated by heating the petroleum coke at 400 °C under air for 1 h to remove any volatile compounds. Five grams of dried petroleum coke was then mixed with dry KOH at mass ratios of 0.5:1, 1:1, 2:1 and 3:1. The mixture was placed in stainless steel crucibles and heated at 40 °C/min to 400 °C under nitrogen (2 L/min) and held at that temperature for 30 min to melt the KOH, increasing contact and converting KOH to K_2O as shown in Eq (1), [23,24].

$$2KOH_l \rightarrow K_2O_l + H_2O_g \quad (1)$$

The samples were then activated by continued heating of the sample under nitrogen atmosphere at a rate of 90 °C/min to temperatures between 800 °C and 950 °C. Samples were held at these temperatures for 15 min unless otherwise specified. When the product cooled to room temperature after the single cycle activation, additional cycles followed. These consisted of the unwashed product of the single cycle activation being exposed to atmosphere, crushed and remixed with no additional chemical reagents. The activation heating cycle was then repeated, once again rising to the activation temperature under an inert atmosphere. The samples were then either put through the washing procedure or were exposed to further heating cycles. The washing process used 20 mL of water per gram of unwashed activated product followed by vacuum filtration. The pore widened activated carbon (PWAC) was then dried at 110 °C overnight. The bulk activated carbon used was produced from a rotary furnace with a feed weight of 8.70 kg. There the petroleum coke was ground to particle sizes less than 0.308 mm and pretreated by heating the petroleum coke at 400 °C under air for 1 h to remove any volatile compounds. The petroleum coke was then mixed with KOH at a 1:1 ratio and run through a rotary furnace under an inert nitrogen atmosphere at 400 °C for 30 min followed by 15 min in the heating zone of the rotary furnace at 900 °C. The samples were then cooled and washed as per the above procedure. These samples were labeled bulk single cycle and were used solely for the oxidation experiments.

2.3. Pore widening mechanism experiments

To elucidate the mechanism of pore widening several experiments were completed. The first isolated the physical effects from the effects of exposure to an oxidizing atmosphere.

For these experiments, typically, 8 g petroleum coke was mixed with 8 g KOH then heated to 400 °C at a rate of 40 °C/min and held at 400 °C for 30 min. This was followed by a heating cycle where the temperature of the oven was increased at a rate of 90 °C/min to 900 °C where it was held for 15 min. Samples were cooled to 25 °C and held for 60 min either with or without an inert nitrogen atmosphere, then the initial cycle conditions were repeated twice. All heat cycles were done under a nitrogen flow rate of 15 L/min. A third sample set had identical activation conditions but was physically ground along with exposure to air in between cycles. All samples were run in triplicate on the Tristar II plus for pore size distribution and specific surface area analysis.

To probe the role of oxidation of the carbon substrate, bulk activated carbon that had been washed was mixed with KOH at a 3:1 ratio both with and without a prior oxidation treatment. Oxidation treatment prior to activation was carried out as follows: 8 g of the activated carbon was added to 120 mL of an oxidizing solution of 2.0 M ammonium persulfate in 1.0 M sulfuric acid. The mixture was stirred at 60 °C for either 1 or 4 h. The mixture was cooled to room temperature and filtered by vacuum filtration. The product was washed with deionized water until the filtrate was approximately neutral, then the collected solid was dried in a vacuum oven overnight at 110 °C. Following this both bulk single cycled activated carbon and oxidized bulk single cycled activated carbon were treated with the following conditions: 3 g AC or oxidized AC was mixed with 9 g KOH and heated to 400 °C at a rate of 40 °C/min where it was held for 30 min. This was followed by a heat cycle where the temperature was increased at a rate of 90 °C/min to 900 °C, where it was held for 15 min. No subsequent cycles were added. A full schematic of all methods can be seen in Figs. S1–4. All samples were run in triplicate for pore size distribution and specific surface area analysis.

2.4. Naphthenic acid adsorption test

The individual adsorption kinetics of the three model naphthenic acids, namely, diphenyl acetic acid (DPA), cyclohexane acetic acid (CHA), and heptanoic acid (HA) were determined on three separate 1:1 KOH:PC activated carbons, that were single, double, and triple cycled. Each activated carbon was sieved to a size between 0.1 mm and 0.3 mm to ensure comparability of samples. Each NA adsorbate solution had an initial concentration of 40 mg/L buffered at pH 8 with a 0.01 M phosphate buffer. 100 mL of the adsorbate solutions was contacted with 50 mg ± 0.5 mg of activated carbon for a period of between 5 min and 48 h at fixed time intervals. Samples were continuously agitated on a shaker table at 200 rpm in sealed glass beakers and filtered into TOC sample vials using 0.45 μm syringe filters to determine residual NA carbon content in the solutions after filtration via a Shimadzu TOC VCPH analyzer using NPOC analysis. The NA adsorbed on the AC was determined by use of the material balance equation, as given by Eq (2) or by percentage of removal given by Eq (3).

$$q_e = \left(\frac{C_0 - C_t}{m}\right) V \quad (2)$$

$$\%removal = \frac{(C_0 - C_t)}{C_0} * 100 \quad (3)$$

Where q_e is the adsorption capacity in mg C/g, C_0 and C_t are the initial TOC and time dependent concentrations (mg C/L) at a given time respectively, and m and V are the masses of AC and volume of solution used.

The analysis of the NA adsorption kinetics was accompanied by mathematical modelling using several commonly used kinetic models. Namely, the pseudo first order, pseudo second order, and Elovich model. However, in all cases, none of the commonly used kinetic models could adequately represent the adsorption kinetics of the model NA species. Instead we explored the use of the multi-exponential equation (m-exp) [25]. The m-exp model, is often used when simpler kinetic models fail to represent experimental data. In the case of our data, the m-exp model is most appropriate as the main purpose of this modelling analysis was to determine half-times of

adsorption. A more detailed description of the *m*-exp modelling analysis can be found in the supplementary information along with an example of adsorption kinetics fitted to the *m*-exp model in Fig. S7.

2.5. Characterization

Specific surface area and pore size distribution analysis was measured using a Micromeritics Tristar II plus with Tristar II Plus v3.02 software. The samples were analyzed using N_2 adsorption at 77 K with 104 points monitoring adsorption and desorption between 0.0065 p/p^0 and 0.995 p/p^0 and 52 points desorption between 0.995 p/p^0 and 0.104 p/p^0. Some samples were additionally investigated using CO_2 adsorption at 273 K. All specific surface areas are reported using Brunauer-Emmet-Teller (BET) specific surface area

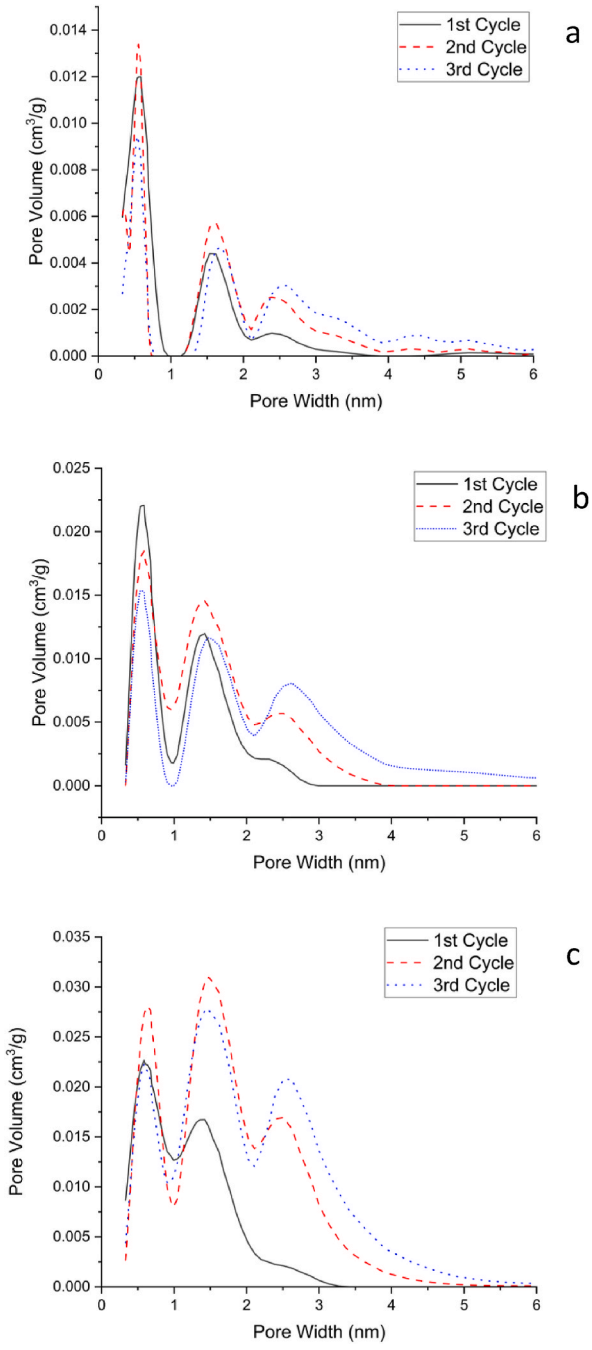

Fig. 1. The incremental pore size distribution of samples activated at a ratio of a) 0.5:1, b) 1:1 c) 2:1 after heating cycles 1, 2 and 3 at 900 °C.

analysis with pore size distributions determined using density functional theory (DFT) with slit geometry modeling 2D-NLDFT with N_2 carbon finite pores. Microporosity was measured using T-plot with points between 0.35 and 0.5 nm using the Harkins and Jura thickness curve [26]. Total pore volume was taken from the single point adsorption from the isotherm. Mesoporosity is taken as the difference between the total pore volume and the micropore volume. Mesoporosity percent is the mesoporosity volume divided by the total pore volume.

The X-ray photoelectron spectroscopy (XPS) analyses were carried out with a Thermofisher Scientific K(alpha) spectrometer using a monochromatic Al K(alpha) source (15 mA, 15 kV). The instrument work function was calibrated using sputter cleaned Au, Ag and Cu to determine the absolute linearity of the binding energy scale, with 83.96 eV for the Au 4f7/2 line for metallic gold, 368.21 eV for Ag

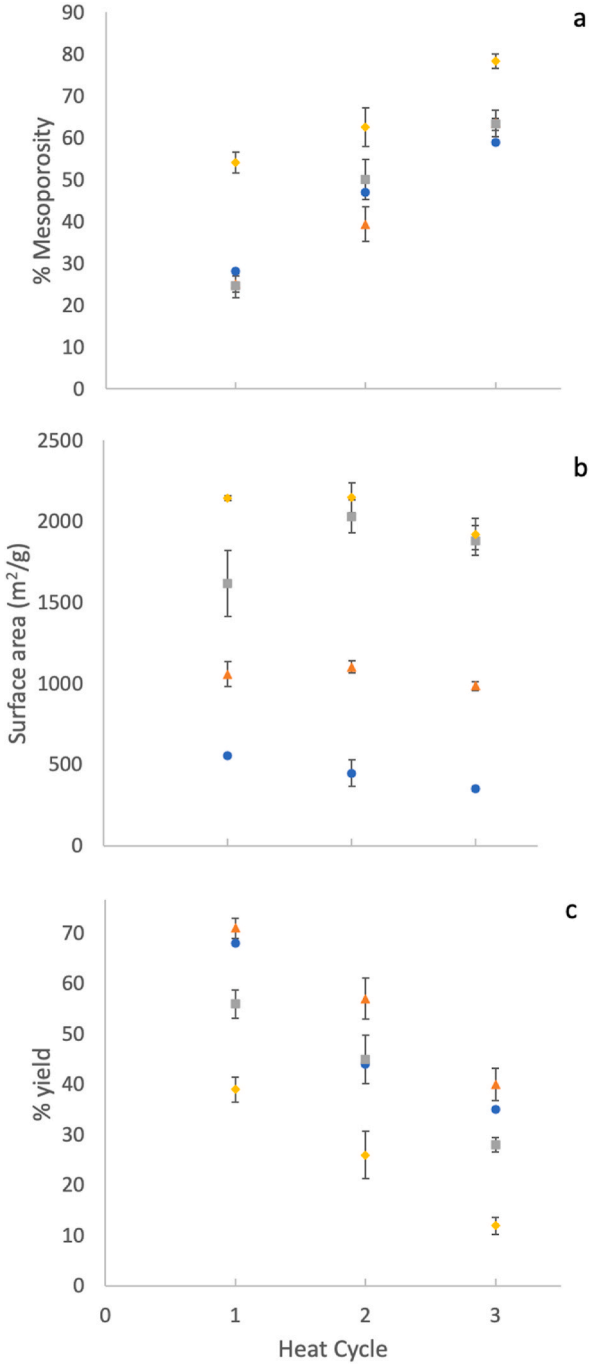

Fig. 2. Effect of cycling and ratio of KOH (0.5:1(●), 1:1 (▲), 2:1 (■), 3:1 (◆)) to petcoke at 900 °C on Activated Carbon cycling, on (a) % mesoporosity, (b) specific surface areas and, (c) Percent yield.

3d5/2, and 932.62 eV for the Cu 2p3/2 line of metallic copper. Survey scan analyses were carried out with a 200 eV pass energy and 1 eV/step. The x-ray spot size is a 2:1 ellipse with a 400 μm major axis. High resolution analyses were carried out with an analysis area of 300 × 700 μm and a pass energy of 20 eV. Fitting was done using CASA XPS (version 2.31) with the spectra being corrected to the main line of the carbon 1s spectrum at 284.85 eV.

The point of zero charge was measured using the pH drift method where 0.01 M NaCl solution was bubbled with N_2 for 10 min. Solutions were adjusted to pH 2, 4, 6, 8 and 10 with 0.1 M HCl and 0.1 M NaOH. 0.150 g of AC was added to each 50 mL aliquot and shaken in an airtight container at 200 rpm for 24 h. The samples were filtered, and the final pH was taken [27,28].

3. Results and discussion

3.1. Effect of heat cycling on porosity

Allowing the unwashed product of the single activation cycle to be reintroduced to subsequent heating cycles after cooling and exposure to air resulted in pore widening with each successive cycle. This is clearly shown by the decrease in the peak intensity at 0.65 nm and the increase in both breadth and intensity for the peaks at 1.5 and 2.7 nm (Fig. 1). This shift to wider pores is seen in Fig. 1a–c, for each of the three KOH:Petcoke ratios examined. This shift can also be seen in the N_2 isotherms (Fig. S5). With each cycle to 900 °C the corresponding % mesoporosity (Fig. 2a) for a 1 KOH:1 PC ratio grew from 25, to 39 to 63. The rise in mesoporosity is the result of a widening of the pores and not the introduction of new porosity, demonstrated by the shifting porosity to the right, which is seen for all activated carbon materials made using different ratios of potassium hydroxide to petcoke.

XPS of samples which underwent first, second and third cycles showed almost identical oxygen and carbon speciation with only slight reductions in C–OH and C–*O*–C bonding (Figs. S6a–d). This points to the surface chemistry remaining unchanged and therefore any changes in adsorption can be attributed to surface morphology. The point of zero charge for first, second and third cycles were 7.8, 8.1 and 7.8 indicating a positively charged surface in which little change took place between cycles. This is consistent with the observed XPS results for surface functionality.

The compiled specific surface areas for the ratios 0.5:1, 1:1, 2:1 and 3:1 of w/w KOH:PC is seen in Fig. 2b. The lower ratio of 0.5:1 saw a small loss in specific surface area between the first and second cycle. While the 1:1 ratio showed pore widening as well as a small change in specific surface area through the heating cycles 1059 ± 75 m^2/g, 1103 ± 37 m^2/g, and 986 ± 27 m^2/g respectively, the 2:1 ratio saw a large jump in specific surface area and pore widening, from 1618 m^2/g to 2032 m^2/g between the first and second cycle. The 3:1 ratio showed a similar increase in mesoporosity going from a single cycle AC with 54% mesoporosity to a three cycle AC with 78% mesoporosity. It underperformed in specific surface area for such a high KOH content with only 1923 m^2/g, a similar specific surface area to that of the 2:1. It also decreased the yields (Fig. 2c) to less than 10%.This demonstrates the impact of the initial ratios of KOH to PC. Heating cycles of as many as 4 and 5 were also explored and did show an increase in mesoporosity, but also demonstrated a continued reduction in yield with every cycle and were not explored further.

To demonstrate that the pore widening was not due solely to an increase in heating time, the results were compared to those obtained for samples formulated using longer single cycle activation times. The results are shown in Fig. 3. Even with an 8-fold increase in activation time to 240 min at 900 °C, there was only a 10% increase in mesoporosity with a 47% yield. This is much lower than the observed 14.3% increase in mesoporosity and 57% yield of the 2 cycle heat treatment seen in Fig. 2 (30 min total time at 900 °C). This excludes the increased activation time as being solely responsible for the effects seen from heat cycling. The cycling is essential for the observed pore widening.

There is a drop in total yield of approximately 15% with each subsequent cycle (Fig. 2c). In an effort to explore methods to mitigate this loss, two approaches were taken: one was to perform subsequent heat treatments at lower temperatures and the second was to try temperature cycling with no hold times (a hold time being the amount of time the samples are held at the target temperature). Lower temperatures (Table 1) of 600 °C, and 700 °C showed no pore widening.

Cycling to 800 °C resulted in some pore widening but with no improvements in yield. Simply cycling to 900 °C with no hold times

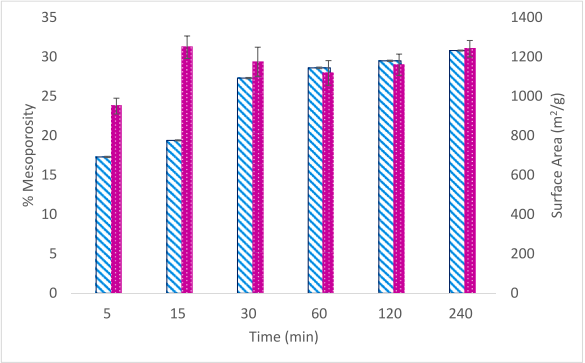

Fig. 3. Specific surface area and percent mesoporosity of activated carbon produced at a ratio of 1KOH:1 PC over increasing time periods.

(NH) (Table 2) produced higher yields but with corresponding smaller shifts in pore widening compared to the longer 15-min hold time. A longer hold time of 30 min produced lower yields and no increase in pore widening suggesting a plateau after 15 min. Tables 1 and 2 summarize these results which show that lower activation temperatures produced no benefits when cycling and that a minimum time needs to be held at temperature for the effects to be produced.

A second heat cycle after washing resulted in an increase of 12 from 38% to 50% in the fraction of the porosity which is mesoporous. This is an increase in the mesoporosity from that of a single cycle AC, but subsequent heating cycles showed much smaller increases in than the unwashed samples. This is likely due to the residual carbon-oxygen species within the pores after the first cycle reacting and burning off. This explains the lack of subsequent increases in mesoporosity for the washed AC that is heat cycled. The comparison of washed and unwashed samples after three heating cycles is shown in Fig. 4.

While the mesoporosity on the AC that is heat treated after washing does show an increase from 21% to 44%, the overall effect on the mesoporosity is much greater for those samples which were not washed between cycles with an increase from 21% to 64% mesoporosity. Both samples lost some total specific surface area which can be related to the loss in microporosity as adjacent pores collapse into one another to form larger mesopores resulting in lower overall specific surface areas.

Different processes could be expected to contribute to the pore widening. Chemical activating agents and activation by-products including K_2O, intercalated K and K_2CO_3 remain in the material following a single activation cycle and are valuable to the pore widening, as evidenced by the reduced pore widening observed when the activated carbon material is washed following the single activation cycle (see Fig. 4). However, even following washing, subsequent thermal treatment yields some pore widening which indicates that other processes also contribute.

If the mechanism of pore widening was purely a physical one resulting from thermal-cracking then cycling under completely inert conditions would have the same effect as experiments where the samples were cycled to room temperature and exposed to atmosphere before being heated again. As the mesoporosity from the single activation cycle is 0.147 cm^3/g (Table 3) and the mesoporosity in the triple cycled inert atmosphere is 0.150 cm^3/g, it can be stated that the inert conditions produced no pore widening and that the mechanism is not a purely physical-mechanical one. It is only when the AC was exposed to an oxidizing atmosphere prior to a heating cycle that the pore widening occurred showing that the introduction of oxygen is essential.

After the single activation cycle much of the potassium is converted to the less active potassium carbonate, and potassium sulfate which upon subsequent heating cycles may also contribute to pore widening [29]. Because of the inert conditions, some of the potassium remains as potassium metal after activation. After exposure to air this potassium metal which is still trapped within the carbon, can spontaneously react to form potassium oxides as shown in equations (4) and (5) [23,30].

$$2K_{(s)} + O_{2\ (g)} \rightarrow\ K_2O_{2\ (s)} \tag{4}$$

$$K_2O_{2\ (s)} + O_{2\ (g)} \rightarrow 2\ KO_{2\ (s)} \tag{5}$$

This introduces oxygen into the activated carbon that can react with the carbon in the subsequent heating cycles. The difference in the shifts of micro to mesoporosity of samples held under inert conditions to those samples that were cycled and exposed to an oxidizing atmosphere are also shown in Fig. 5, with the latter showing the peak at 1 nm decreasing and the peaks at 2 and 3–4 nm widening and increasing in height. The difference between the ground and unground samples can be attributed to the increased exposure to air that occurs when samples are ground in ambient conditions.

To further investigate the role of oxygen in pore widening, an oxidized activated carbon and a standard activated carbon underwent a second activation by mixing the AC with KOH at a ratio of 3KOH:1AC. The objective here was to explore the role that the extent of oxidation of the carbon substrate plays in the pore widening mechanism. It is not possible to oxidize the activated carbon following the single activation cycle without removing residual potassium activating species which, as demonstrated above, we know to be necessary for the pore widening process. Thus, post oxidation of single cycle activated carbon was followed with additional inputs of KOH to furnish the necessary potassium species for the subsequent heating process. This rather high KOH to AC ratio was chosen to magnify any effects in the role that carbon surface oxidation plays. The oxidation of the AC showed no increase in mesoporosity, and as seen consistently in literature, lost specific surface area. The heat cycling of both the standard activated carbon, and the oxidized activated carbon without additional KOH had no real increase in mesopore volume. The subsequent second activation with additional KOH of the AC with and without oxidation both resulted in large increases in mesoporosity as shown in Table 4. The re-activated oxidized AC did experience a larger change especially in the 3–4 nm range (Fig. 6) with a total increase in mesopore volume of 0.285 cm^3/g as opposed to the 0.227 cm^3/g of the standard re-activated AC. This difference can be attributed to the increase in oxygen content on the

Table 1
Effect of 1KOH:1 PC at 900 °C with lower subsequent activation temperatures on specific surface area and pore size distribution.

Number of activation cycles	2nd Cycle Temp. (°C)	1st Cycle time (min)	Total time (min)	Surface Area (m^2/g)	Standard Deviation (m^2/g)	Mesoporosity (%)	Standard Deviation (%)	% Yield
1	–	15	15	1059	75	25.1	2.3	71
2	900	15	30	1103	37	39.4	0.2	57
3	900	15	45	986	27	63.5	2.1	40
2	800	15	30	1034	88	38.2	3.2	53
3	800	15	45	733	–	50.1	1.1	41
2	700	15	30	930	–	25.5	1.2	61
2	600	15	30	815	17	25.6	1.6	61

Table 2
Effect of no hold times on subsequent heating cycles surface area and pore size distribution of activated carbon (1KOH:1 PC 900 °C).

Number of Cycles	2nd Cycle Temp. (°C)	1st Cycle Time (min)	Total Time (min)	Surface Area (m^2/g)	Standard Deviation (m^2/g)	Mesoporosity (%)	Standard Deviation (%)	Yield (%)	Standard Deviation (%)
1	_	15	15	1059	75	25.1	2.3	71	0.6
2	900	15	15 + NH	1034	88	43.2	3.2	53	1.8
3	900	15	15 + 2 NH	930	11	56.6	1.6	48	2.2
1	900	30	30	1217	25	23.4	0.2	64	3
2	900	30	60	1167	25	43.1	2.3	48	1
3	900	30	90	1084	238	61.2	2.0	34	1

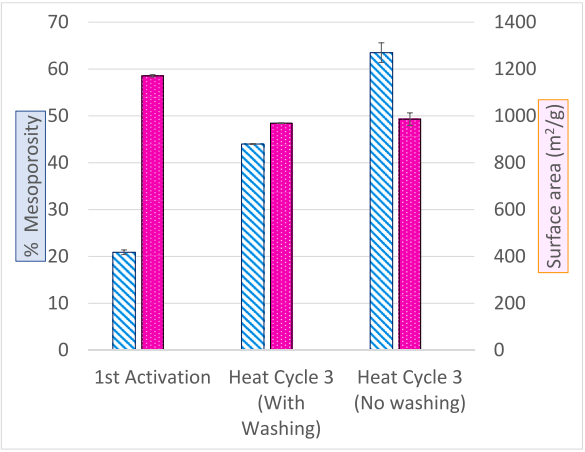

Fig. 4. Specific surface areas and % mesoporosity of activated carbons produced at 1KOH: 1PC ratios at 15 min and then heat treated twice at 900 °C after 1st activation was washed and unwashed.

Table 3
Specific surface areas and pore volumes of AC's investigated for the impact of oxidation between cycles on mesoporosity.

Sample	Surface area (m^2/g)	Total Pore Volume (cm^3/g)	Micropore Volume (cm^3/g)	Mesopore Volume (cm^3/g)	Mesoporosity (%)	% yield
Single cycle AC	1382± 49	0.557 ± 0.019	0.410 ± 0.011	0.147 ± 0.030	26	74 ± 8
3 cycles 1KOH:1 PC Intermediate inert atmosphere and no intermediate mixing	1391 ± 16	0.558 ± 0.006	0.407 ± 0.007	0.150 ± 0.014	27	65 ± 1
3 cycles 1KOH:1 PC Intermediate air exposure and no intermediate mixing	1210 ± 13	0.521 ± 0.007	0.299 ± 0.007	0.221 ± 0.013	43	51 ± 3
3 cycles 1KOH:1 PC Intermediate air exposure and intermediate mixing	1339 ± 21	0.654 ± 0.023	0.324 ± 0.031	0.330 ± 0.054	50	54 ± 2

carbon surface as measured by XPS which went from 8 atomic % oxygen in the AC to over 22% oxygen in the oxidized AC. At 900 °C this oxygen is reacting with the surface of the AC to form CO_2 and CO thus further hollowing out existing porosity resulting in pore widening. The pore widening of the 3 KOH: 1 AC can be attributed solely to the oxygen introduced via the KOH. It should be noted that the total specific surface area of what would be cumulatively larger than a 4KOH:1 PC has a much smaller total specific surface area than what would be formed in a single activation cycle. The additional KOH is failing to form new porosity most likely due to the annealing effect of activation and is only hollowing out existing porosity further.

In summary, pore widening of cycled activated carbon can be attributed to the oxidation of potassium metal and the carbon surface and its subsequent reaction within existing pores at high temperatures. To increase mesoporosity further, treatments of the surface which add reactive oxygen groups create a further widening of existing porosity.

3.2. Effect of increased mesoporosity on kinetics of adsorption of naphthenic acids

As a demonstration of the effect of pore widening on the adsorption behavior of the PWAC, we have explored the uptake of 3 model

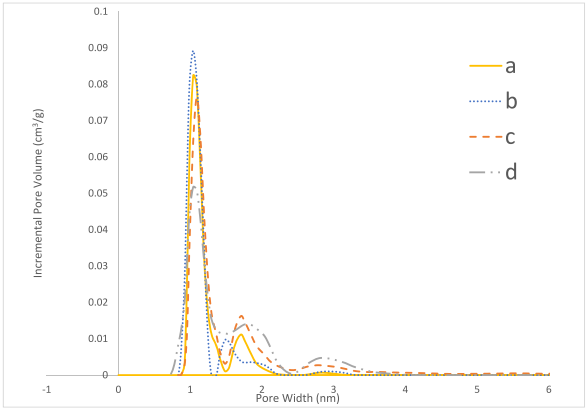

Fig. 5. Incremental pore volume distribution of samples run through a) single cycle activation and b) 3 heat cycles with a continual inert atmosphere and no mixing in between cycles, c) 3 heat cycles with exposure to atmosphere in between cycles and no mixing, and d) 3 heat cycles with exposure to atmosphere in between cycles and mixing.

Table 4
Specific surface areas and pore volumes of AC's investigating the impact of surface oxidation on pore widening.

Sample	Surface Area (m^2/g)	Total Pore Volume (cm^3/g)	Micropore Volume (cm^3/g)	Mesopore Volume (cm^3/g)	Mesoporosity (%)
Blank AC	960 ± 30	0.393 ± 0.013	0.276 ± 0.011	0.118 ± 0.024	30
Single cycle AC + 1 heat cycle	1056 ± 89	0.436 ± 0.037	0.291 ± 0.031	0.145 ± 0.068	33
Oxidized AC 1hr	858 ± 13	0.354 ± 0.005	0.245 ± 0.004	0.109 ± 0.008	31
Oxidized AC + 1 heat cycle	616 ± 26	0.248 ± 0.012	0.185 ± 0.006	0.063 ± 0.018	25
3 KOH: 1 oxidized AC	871 ± 84	0.454 ± 0.050	0.051 ± 0.003	0.403 ± 0.053	89
3KOH: 1 AC (no oxidation)	1032 ± 50	0.493 ± 0.027	0.148 ± 0.001	0.345 ± 0.028	70

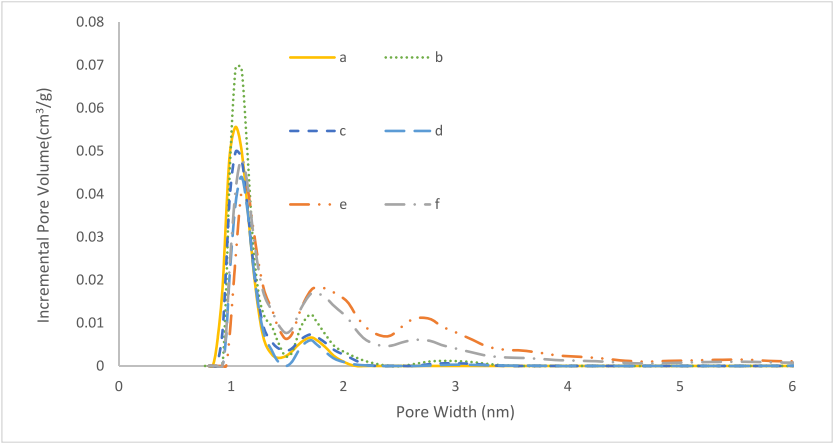

Fig. 6. Incremental pore volume distribution of samples run through a) one standard activation, b) 1 additional heat cycle of washed AC, c) AC oxidized 1 h, d) AC oxidized with one additional heat cycle, e) 3KOH:1AC with one cycle, and f) 3KOH: 1AC oxidized with one heat cycle.

naphthenic acids since the remediation of NAs from OSPW is paramount to the potential release of processed waters from tailings ponds and its in-process recycling.

As shown in Fig. 7, adsorption equilibrium is achieved within approximately 24 h for each model NA. For a given model NA, minimal difference in adsorption capacity at equilibrium is seen when comparing results for the single, double and triple cycled PWAC. However, consistent visual differences in the initial rate of adsorption, with minor exceptions, are observed in Fig. 7.

When adsorption capacity is normalized to specific surface area of the activated carbons used to account for slight differences in specific surface area, as shown in Fig. 8a–c, clearer differences in the initial kinetics of adsorption are observed. For all three model NAs investigated, initial adsorption kinetics on the triply heat-cycled PWAC was consistently the fastest, followed by adsorption on the

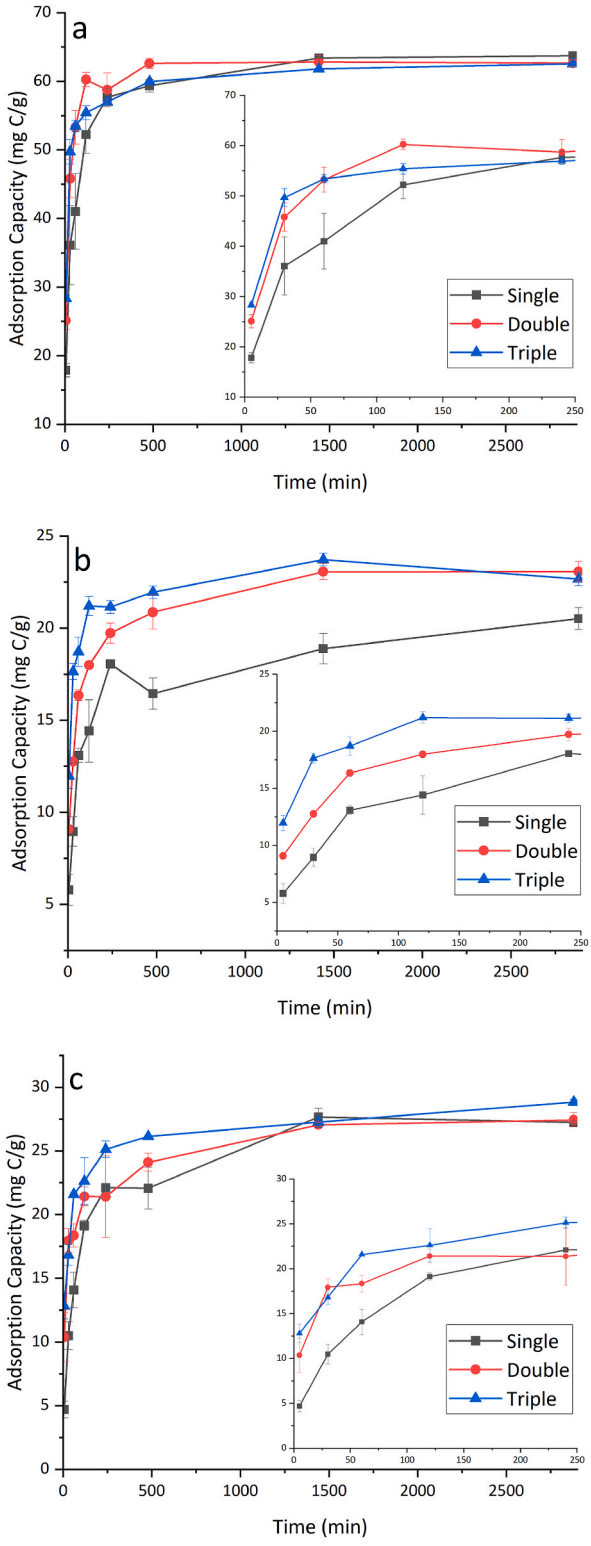

Fig. 7. Adsorption kinetic plots showing adsorption (mg C/g) versus time for each model NA on each activated carbon tested, along with an inset showing the initial adsorption up to 2 h (a) diphenylacetic acid (DPA), (b) cyclohexane acetic acid (CHA) and (c) heptanoic acid (HA).

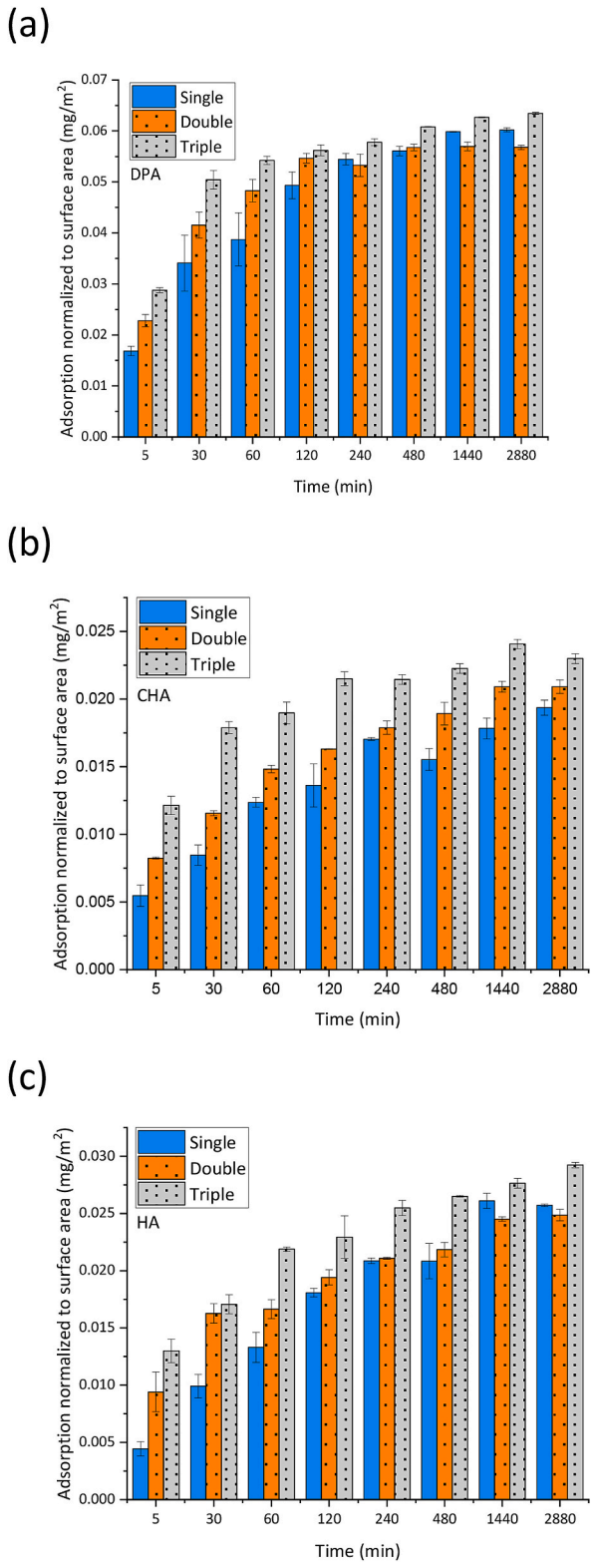

Fig. 8. Adsorption Kinetics with adsorption capacity normalized to total specific surface area of each activated carbon used for (a) diphenylacetic acid (DPA), (b) cyclohexane acetic acid (CHA) and (c) heptanoic acid (HA).

double, then on the single cycled PWAC. The most significant difference between the surface characteristics of these three activated carbons is the distribution of porosity, with the single, double, and triple cycled PWAC having a percentage of mesoporosity of 25.1 ± 2.3, 39.4 ± 0.2, and 63.5 ± 2.1 respectively. The differences in adsorption kinetics observed for a given model NA seen in the single, double, and triple cycled PWAC are consistent with the increase in mesoporosity identified in these three activated carbons. Increased mesoporosity is expected to improve the internal diffusion of adsorbate within activated carbon to reach their ultimate adsorption sites within the microporous space.

To further emphasize the differences in the initial kinetics of adsorption observed in Fig. 7, kinetic modelling using the *m*-exp model was also performed. Error analysis, as displayed in Table S1 in the supplementary material, demonstrated adequate *m*-exp model fitting for all adsorption kinetics plots. To adequately represent each adsorption kinetics system, three summed expressions within the *m*-exp model equation were required. The fitting constants for each adsorption system can also be found in the Supplementary Material Table S2. Using the *m*-exp fitted parameters, the resulting kinetic model was used to determine adsorption half times ($t_{1/2}$), which are presented in Table 5.

A noticeable decrease in $t_{1/2}$ values were observed for each model NA from single, double to triple cycled PWAC. A minor exception to this was observed in the case of heptanoic acid (HA) $t_{1/2}$ values in the double versus triple cycled PWAC. However, a significant reduction in $t_{1/2}$ in the single versus double cycled PWAC was still clearly observed for the heptanoic acid. These reductions in adsorption $t_{1/2}$ are a strong demonstration of how the increase in mesoporosity, achieved with multiple heating cycles, improves the adsorption kinetics.

4. Conclusion

Each activation cycle of unwashed KOH activated petcoke at 900 °C, resulted in a significant shift towards increased mesoporosity. This has been demonstrated for all ratios of KOH, from 0.5:1 to 3:1. The cycling resulted in as much as a 38.5% increase in mesoporosity with a 20% drop in yield without additional chemical or physical inputs of activating agents.

Heat cycles after product washing also showed pore widening but to a much lesser extent than the unwashed cycling products. A cycling temperature of 800 °C resulted in some increase in mesoporosity while lower temperatures of 600 °C and 700 °C resulted in none, with 900 °C showing the best results. The impact of this pore widening effect was demonstrated with adsorption of three sample naphthenic acids. The resulting kinetics modelling using the *m*-exp model show a significant reduction in adsorption half-time with the increasing number of activation cycles [25]. This improvement is ascribed to the increase in mesoporosity achieved by activation cycling.

Repeated heat cycling of the unwashed activated product is a convenient, cost efficient and effective means of improving mesoporosity and by extension the adsorption performance of KOH activated carbons, without increased chemical inputs.

Author contribution statement

Oliver K.L. Strong, Elmira Nazari, Tyler Roy: Conceived and designed experiments; Performed experiments; Analyzed and interpreted data; Wrote the paper.

Kevin Scotland: Analyzed and interpreted data; Wrote the paper.

Paul R. Pede: Conceived and designed the experiments; Contributed reagents, materials, analysis tools or data.

Andrew J. Vreugdenhil: Conceived and designed the experiments; Contributed reagents, materials, analysis tools or data; Wrote the paper.

Funding statement

This research did not receive any specific grant from funding agencies in the public, commercial, or not-for-profit sectors.

Data availability statement

Data will be made available on request.

Declaration of interest's statement

The authors declare no conflict of interest.

Table 5
Adsorption half times for model NAs onto each activated carbon tested based on m-exp modelling. Adsorption half times ($t_{1/2}$) are in minutes.

$t_{1/2}$	Single Cycled PWAC	Double Cycled PWAC	Triple Cycled PWAC
DPA	20.0	8.4	6.6
CHA	34.3	18.5	4.5
HA	51.4	8.7	12.0

Appendix A. Supplementary data

Supplementary data to this article can be found online at https://doi.org/10.1016/j.heliyon.2023.e13500.

References

[1] M. Sevilla, R. Mokaya, Energy storage applications of activated carbons: supercapacitors and hydrogen storage, Energy Environ. Sci. 7 (2014) 1250–1280.
[2] H.S. Niasar, et al., Preparation of activated petroleum coke for removal of naphthenic acids model compounds: box-Behnken design optimization of KOH activation process, J. Environ. Manag. 211 (2018) 63–72.
[3] N. Arena, J. Lee, R. Clift, Life Cycle Assessment of activated carbon production from coconut shells, J. Clean. Prod. 125 (2016) 68–77.
[4] U. Beker, H. Dertli, D. Duranoglu-Gulbayir, R.D. Cakan, Study of cherry stones as a precursor in the preparation of low cost carbonaceous adsorbent, Energy Sources, Part A Recovery, Util. Environ. Eff. 32 (2010) 1004–1015.
[5] R.M. Teare, et al., St98, 2021, p. 2012.
[6] R. Puente-Ornelas, C.J. Lizcano-Zulaica, A.M. Guzmán, P.C. Zambrano, T.K. Das-Roy, Dissolution of refractories for gasification process of petroleum coke for the steel industry, Fuel 93 (2012) 581–588.
[7] J. Huang, et al., Functionalization of petroleum coke-based mesoporous carbon for synergistically enhanced capacitive performance, J. Mater. Res. 32 (2017) 1248–1257.
[8] S.E. Chun, J.F. Whitacre, Formation of micro/mesopores during chemical activation in tailor-made nongraphitic carbons, Microporous Mesoporous Mater. 251 (2017) 34–41.
[9] M.A. Lillo-Ródenas, D. Lozano-Castelló, D. Cazorla-Amorós, A. Linares-Solano, Preparation of activated carbons from Spanish anthracite - II. Activation by NaOH, Carbon N Y 39 (2001) 751–759.
[10] J.H. Kim, D. Lee, T.S. Bae, Y.S. Lee, The electrochemical enzymatic glucose biosensor based on mesoporous carbon fibers activated by potassium carbonate, J. Ind. Eng. Chem. 25 (2015) 192–198.
[11] L.D. Virla, V. Montes, J. Wu, S.F. Ketep, J.M. Hill, Synthesis of porous carbon from petroleum coke using steam, potassium and sodium: combining treatments to create mesoporosity, Microporous Mesoporous Mater. 234 (2016) 239–247.
[12] P.V. Kugatov, I.I. Bashirov, B.S. Zhirnov, Production of a mesoporous carbon adsorbent from carbon black and petroleum pitch by high-temperature roasting and steam activation, Coke Chem. 59 (2016) 345–348.
[13] J. Wu, V. Montes, L.D. Virla, J.M. Hill, Impacts of amount of chemical agent and addition of steam for activation of petroleum coke with KOH or NaOH, Fuel Process. Technol. 181 (2018) 53–60.
[14] M. Yan, et al., Micro-mesoporous graphitized carbon fiber as hydrophobic adsorbent that removes volatile organic compounds from air, Chem. Eng. J. 452 (2023).
[15] I. Campello Gómez, O.F.B. Cruz, J. Silvestre-Albero, C.R. Rambo, M. Martinez Escandell, Role of KCl in activation mechanisms of KOH-chemically activated high surface area carbons, J. CO2 Util. 66 (2022) 2212–9820.
[16] A.M. Cancelli, F.A.P.C. Gobas, Treatment of naphthenic acids in oil sands process-affected waters with a surface flow treatment wetland: mass removal, half-life, and toxicity-reduction, Environ. Res. 213 (2022).
[17] J.V. Headley, D.W. McMartin, A review of the occurrence and fate of naphthenic acids in aquatic environments, J. Environ. Sci. Health A Tox Hazard Subst. Environ. Eng. 39 (2004) 1989–2010.
[18] L.S. Migliorin, et al., Application of mesoporous zeolite Socony Mobil-5 (ZSM-5) as an adsorbent material for the removal of naphthenic acid present in oil-produced water, Microporous Mesoporous Mater. 344 (2022).
[19] H.S. Niasar, H. Li, T.V.R. Kasanneni, M.B. Ray, C.C. Xu, Surface amination of activated carbon and petroleum coke for the removal of naphthenic acids and treatment of oil sands process-affected water (OSPW), Chem. Eng. J. 293 (2016) 189–199.
[20] H. Seyedy Niasar, Dr C. Xu, Chunbao), Dr M. Ray, Treatment of oil sands process-affected water using activated and surface modified petroleum coke for organic compounds recovery, Chemical and Biochemical Engineering (2017) 190. Chem. Biochem. Engin.
[21] F.S. Azad, J. Abedi, S. Iranmanesh, Removal of naphthenic acids using adsorption process and the effect of the addition of salt, J. Environ. Sci. Heal. Part A Toxic Hazar. Sub. Environ. Engin. 48 (2013) 1649–1654, https://doi.org/10.1080/10934529.2013.815457. Preprint at.
[22] S. Iranmanesh, T. Harding, J. Abedi, F. Seyedeyn-Azad, D.B. Layzell, Adsorption of naphthenic acids on high surface area activated carbons, J. Environ. Sci. Health A Tox Hazard Subst. Environ. Eng. 49 (2014) 913–922.
[23] T. Otowa, Y. Nojima, T. Miyazaki, Development OF KOH activated high surface area carbon and its application to drinking water purification, Carbon 35 (1997).
[24] M. Lillo-Rodenas, D. Cazorla-Amoros, A. Linares-Solanó, U nderstanding chemical reactions between carbons and NaOH and KOH an insight into the chemical activation mechanism, Carbon 41 (2003).
[25] A.W. Marczewski, M. Seczkowska, A. Deryło-Marczewska, M. Blachnio, Adsorption equilibrium and kinetics of selected phenoxyacid pesticides on activated carbon: effect of temperature, Adsorption 22 (2016) 777–790.
[26] J. Jagiello, J.P. Olivier, A simple two-dimensional NLDFT model of gas adsorption in finite carbon pores. application to pore structure analysis, J. Phys. Chem. C 113 (2009) 19382–19385.
[27] L.S. Ćerović, et al., Point of zero charge of different carbides, Colloids Surf. A Physicochem. Eng. Asp. 297 (2007) 1–6.
[28] M.V. Lopez-Ramon, F. Stoeckli, C. Moreno-Castilla, F. Carrasco-Marin, On the characterization of acidic and basic surface sites on carbons by various techniques, Carbon N Y 37 (1999) 1215–1221.
[29] G. Singh, A. Maria Ruban, X. Geng, A. Vinu, Recognizing the potential of K-salts, apart from KOH, for generating porous carbons using chemical activation, Chem. Eng. J. 451 (2023).
[30] M. Lillo-Rodenas, D. Lozano-Castello, D. Cazorla-Amoros, A. Linares-Solanó, Preparation of activated carbons from Spanish anthracite II. Activation by NaOH, Carbon 39 (2001).